Morphological Evolution of Polypropylene/Polystyrene Blends in a Twin-Screw Extruder

Yang Wu,[1,3] Shaowei Jing,[2] Qun Gu,[3] Binyao Li[4]

[1]Institute of Polymers, Nanchang University, 999 Xuefu Ave, Nanchang 330031, People's Republic of China
[2]94th Hospital of People's Liberation Army, Nanchang 330002, People's Republic of China
[3]Ningbo Key Laboratory of Polymer Materials, Polymer and Composites Division, Ningbo Institute of Materials Technology and Engineering, Chinese Academy of Sciences, Ningbo 315201, People's Republic of China
[4]State Key Laboratory of Polymer Physics and Chemistry, Changchun Institute of Applied Chemistry, Chinese Academy of Sciences, Changchun 130022, People's Republic of China

ABSTRACT: The effects of the blend composition and rotation speed on the morphological evolution of polypropylene (PP)/polystyrene (PS) blends were investigated in a twin-screw extruder. When PS was the major component, the rate of melt and the rate of dispersion played final roles in the morphological development of the polymer melts. However, when PP was the major component, the rate of dispersion and the rate of coalescence played key roles. A high tendency to coalesce occurred at a high rotation speed and/or a high content of the dispersed phase. When the PP/PS blend composition was close to 1, a cocontinuous morphology was observed to transmute into a coarse one with increasing rotation speed. Attempts were made to correlate the morphology and mechanical properties. © 2010 Wiley Periodicals, Inc. J Appl Polym Sci 119: 1970–1977, 2011

Key words: blends; mechanical properties; morphology

INTRODUCTION

As the industrial importance of immiscible polymer blends is increasing, it is of crucial importance to understand in detail the fundamental parameters controlling the blend phase morphology during the mixing process because most properties of blends of immiscible polymers depend on the fineness of the phase morphology.[1–10] The effects of the material characteristics (interfacial tension, melt viscosity, melt elasticity, and molecular weight), processing conditions (time of mixing, temperature of mixing, rotation speed, and mixer type), and blend composition on the final blend phase morphology have been studied extensively.[11–16]

The morphological development of immiscible polymer blends is a complex process. Nevertheless, it has generally been observed that under normal thermomechanical conditions, the most significant changes in morphology occur in the initial stage of melt blending (1–2 min) in a batch mixer or in the melting/plastification zone (one-dimensional to three-dimensional) of a twin-screw extruder.[11,12] Potente et al.[13] found that a finely dispersed morphology already formed at the start of the melting section. It did not undergo any essential change as the blend passed through the extruder, and only a limited correlation was evident with the process parameters. However, this might have been because too high a rotation speed was applied. Nair et al.[14] observed that the most significant breakdown occurred at an increasing rotor speed from 9 to 20 rpm in the PS/P6 blends, and the domain size remained almost the same even at higher rotor speeds. Sundararaj and Macosko[15] reported that there was a critical shear rate in polymer systems at which a minimum particle size was achieved. It could be explained by the polymer elasticity. When the shear rate was increased, the matrix viscosity decreased, and the droplet elasticity increased so that the droplet resisted deformation to a greater extent. Joseph and Thomas[16] showed that the domain size increased as the PS content increased in a PS/polybutadiene blend, and this was attributed to reagglomeration or coalescence of the dispersed rubber particles. A finer morphology developed when the dispersed phase had a lower viscosity than the matrix.

In the past, some research groups[17–23] have attempted to model the morphological evolution of immiscible polymer blends during compounding. Macosko's group[17,18] reported that a major reduction in the domain size occurred in conjunction with the melting or

Figure 1 Extruder layout and sampling locations: (A) past the first kneading block, (B) past the second kneading block, and (C) past the third kneading block.

softening of the component and that the initial mechanism of morphological development involved the formation of a sheet or ribbon structure of the dispersed phase. Plochocki et al.[19] studied the processing of PS/low-density polyethylene blends in several industrial mixers and observed that the initial dispersion mechanism might be due to abrasion of solid or partially softened pellets on the wall of the processing equipment. Tyagi and Ghosh[20] considered the size of droplets formed by the breakup of filaments. The final droplet size was governed by the emulsification process occurring as a result of stretching, breakup, and coalescence in the metering section of the screw. Lee and Han[21,22] investigated the evolution of morphology during compounding in an internal mixer and twin-screw extruder and proposed a model for the evolution of the phase morphology. They found that the initial blend morphology depended very much on the difference in T_{cf} (T_{cf} of an amorphous polymer is equivalent to the "melting point" of a crystalline polymer) or the melting temperature between the constituent components and also on the viscosities of the constituent components. They observed that a cocontinuous morphology was formed at the front end of the extruder, and this then transformed into a dispersed morphology toward the end of the extruder. Despite much effort, we still do not have a clear understanding of the morphological evolution mechanism in immiscible polymer blends during compounding in a twin-screw extruder with respect to complex flows.

The objective of this study was to investigate online the morphological evolution of polypropylene (PP)/PS blends in a twin-screw extruder with respect to the influence of the blend composition and rotation speed when PS varies from the major phase to the minor one. Also, the correlation between the morphology and mechanical properties was examined.

EXPERIMENTAL

Materials

The isotactic PP used (1300) had a melt index of 1.5 g/10 min (230°C/2.16 kg), a density of 0.91 g/cm^3, and a

Vicat softening temperature of 160°C. The PS used (666D) had a melt index of 8.0 g/10 min (230°C/2.16 kg), a density of 1.05 g/cm^3, and a Vicat softening temperature of 97°C. They were both supplied by Yan Shan Petrochemical Co. (Beijing, China).

Experimental procedures

The melt blending of neat PP and PS with weight ratios of 90/10, 70/30, 60/40, 40/60, and 20/80 was conducted with a corotating twin-screw extruder (Rheomex PTW24/40P, Haake, Germany) with a length/diameter ratio of 40. The extruder layout and sampling locations are presented in Figure 1. The screw configuration had three kneading blocks and consisted of eight zones with a temperature profile of 180/190/200/210/210/210/210/210°C. Rotation speeds of 40, 80, 120, and 150 rpm were used for every blend pair, and the throughput was 3.5 kg/h. In our experiment, two polymers with a given blend ratio were tumbled in a drum for about 10 min before being fed into the hopper of the extruder. The samples were collected at positions A, B, and C, which had length/diameter ratios of 16, 26, and 34, respectively. The samples were immediately quenched in liquid nitrogen to avoid further morphological changes.

Morphological characterization

The blend specimens were ultramicrotomed with an Ultracut R with an FCS microtome (Wetzlar, Germany) equipped with glass knives under the temperature of −80°C. A transmission electron microscope (JEM 1010, JEOL, Japan), operated at 100 kV, was used to take micrographs of the PP/PS blend specimens. The average diameters of the dispersed particles were quantified with self-made software. The contour and mass center of each particle were detected, and each particle was scanned by straight lines going through the mass center from different directions; the minimum span from one side of a particle to the other was defined as the particle diameter, and consequently, the average size of the particles could be calculated by averaging of
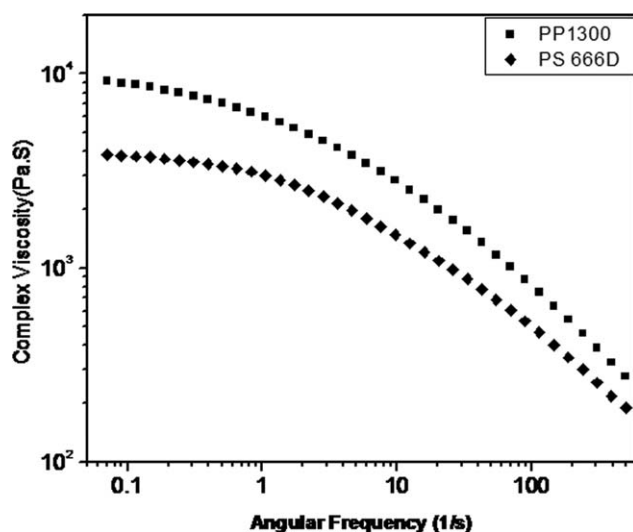
Figure 2 Shear rate dependence of the viscosity of PP and PS at 210°C.

the particle diameter values. To obtain more reliable data, more than 100 particles were considered to calculate these structure parameters for each sample. Furthermore, the average particle diameter (d_n) was calculated on the basis of eq. (1):

$$d_n = \frac{\sum_{i=1}^{\infty} n_i d_i}{\sum_{i=1}^{\infty} n_i} \quad (1)$$

where n_i and d_i is the number and diameter of particles, respectively.

Rheological measurements

Two plates, one for PP and the other for PS, were prepared by compression molding on a glass plate at 200°C. The thickness of each plate was about 1.0 mm, and the diameter was 25 mm. The plates were put into a rheometer (Physica MCR300, Anton-Paar, Germany) at 210°C under a nitrogen environment, and the complex viscosity was measured at shear rates ranging from 0.07 to 500 s^{-1} with an applied strain of 5%. Figure 2 describes the dependence of the viscosity of PP and PS on the shear rate. The viscosity of PP was higher than that of PS over the entire range of shear rates tested.

Mechanical testing of the samples

After mixing, the molten materials from the nozzle were sheeted out. The sheets were removed and pressed in a mold under a hot condition. Compression-molded sheets about 1 mm thick were obtained with a self-made press at 200°C and 500 N/cm^2 for 5 min and then cooled to the ambient temperature in air. The samples for tensile testing were punched out from the molded sheets parallel to the direction of extrusion.

Tensile testing of the samples was performed at the ambient temperature according to the GB/T 1040-1992 test method with dumbbell-shaped test specimens at a crosshead speed of 10 mm/min with an Instron model 1121 testing machine (Canton, MA)

RESULTS AND DISCUSSION

Morphological evolution mechanisms of PP/PS blends with various compositions and rotation speeds

According to Lee and Han,[21,22] the rheological properties of the constituent components, blend composition, and processing variables have a final influence on the morphological evolution in immiscible polymer blends. If the polymer forming the minor phase has a higher melting/softening temperature than the one forming the matrix, Li and Hu[23] considered the most favorable conditions for obtaining a fine morphology to be as follows: rate of melting/plastification of the dispersed phase ≪ rate of dispersion (deformation + breakup) of the polymer melt to small particles ≪ rate of stabilization (with an adequate copolymer) of these small particles.

Figure 3 presents transmission electron microscopy (TEM) micrographs describing the morphological evolution in a 20/80 PP/PS blend along the extruder axis. In all the TEM micrographs, the dark
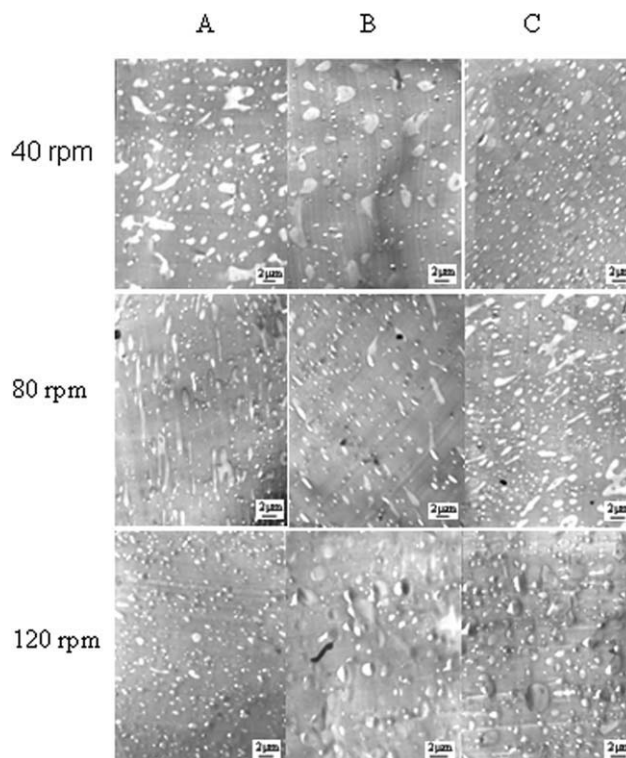
Figure 3 Morphology of 20/80 PP/PS blends during compounding in a twin-screw extruder at the rotation speeds of 40, 80, and 120 rpm.

areas represent PS, and the light areas represent PP. At a rotation speed of 40 rpm, we can clearly observe a dispersed morphology in which the droplets of PP are dispersed in the PS matrix. The size of the droplets decreases from about 1.0 μm (position A, which is downstream of the first kneading block) to 0.8 (position B, which is past the second kneading block) and 0.5 μm (position C, which is past the third kneading block) along the extruder axis. When the rotation speed is increased to 80 rpm, elongated and oriented droplets of PP can be observed. The size of the droplets remains constant at about 0.7 μm. However, the orientation is weakened along the extruder axis. At 120 rpm, the size of the droplets of PP increases from 0.5 μm (position A) to 0.9 (position B) and 1.0 μm (position C).

In Figure 3, we can observe that the size of the droplets decreases at 40 rpm and remains constant at 80 rpm. However, there is a coarseness to the droplets when the rotation speed is increased to 120 rpm. The rate of melting is far greater than the rate of dispersion for a rotation speed of 40 rpm. The content of the melt is too high to be quickly dispersed. Thus, it is a process of size reduction for polymer melts. However, when the rate of melting is lower than the rate of dispersion for a rotation speed of 120 rpm, the droplets generated in the very early stage of melt blending are very small. In fact, the increase in the rotation rate favors both dispersion (mainly for the large droplets) and coalescence (mainly for the small droplets) of the polymer melt. Therefore, the small droplets can coalesce with one another. It is a process of size enhancement.

The morphological development of blends when the volume ratio of PP to PS is close to 1 (PP/PS with a weight ratio of 40/60) is shown in Figure 4. We can observe a cocontinuous morphology at all positions at 40 rpm. When the rotation speed is increased to 80 rpm, the cocontinuous morphology (position A) is transmitted into an elongated and oriented one (positions B and C). At 120 rpm, the elongated and oriented morphology (positions A and B) is transmitted into a coarse one (position C) in which large and irregular droplets of PS are dispersed in the PP matrix. Let us consider the situation in which PP and PS are compounded in a twin-screw extruder. At the front ends of the extruder, PS melts first because of its lower flow temperature. The mixture is a suspension consisting of molten PS, which forms the continuous phase, and solid PP. As the suspension moves along the extruder axis and reaches a temperature at which PP starts to melt, a liquid mixture will form a dispersed morphology, in which droplets of PP are dispersed in the matrix of PS. There are two possibilities: either the same mode of dispersion persists along the rest of the extruder or phase inversion may take place, in which PP
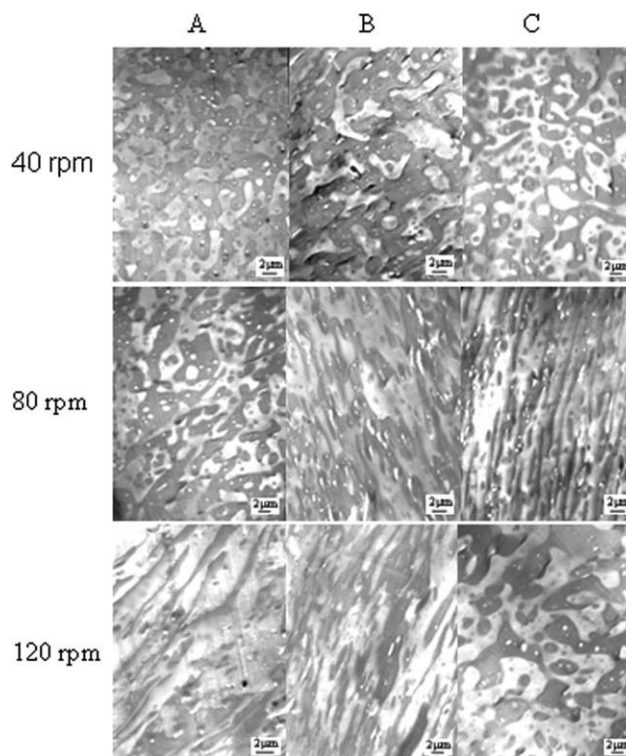

Figure 4 Morphology of 40/60 PP/PS blends during compounding in a twin-screw extruder at the rotation speeds of 40, 80, and 120 rpm, respectively.

becomes the continuous phase and PS becomes the discrete phase. In fact, when PP is the major component, the blend ratio plays a greater role than the viscosity ratio in determining the state of dispersion. Some investigators[21,22] have shown that a cocontinuous morphology is a transitory morphological state through which one mode of a dispersed morphology is transformed into another one, and the transformation can occur by an increase in either the rotation speed of the mixer or the melt-blending temperature. According to the minimum entropy production principle, the more viscous component will form the discrete phase, and the less viscous component will form the continuous phase. Thus, it is reasonable to observe that in 40/60 PP/PS blends, PP forms the discrete phase and PS forms the continuous phase at a high rotation speed.

If the polymer forming the minor phase has a lower melting/softening temperature than the one forming the matrix, how does the morphology of polymer melts develop? Let us observe the morphological evolution in 60/40 and 90/10 PP/PS blends along the extruder axis, as shown in Figures 5 and 6, respectively.

In Figure 5, we find that the PS droplets are elongated and oriented ones at all rotation speeds. For a rotation speed of 40 rpm, the size of the droplets is 0.6 μm at positions A and B. However, we can
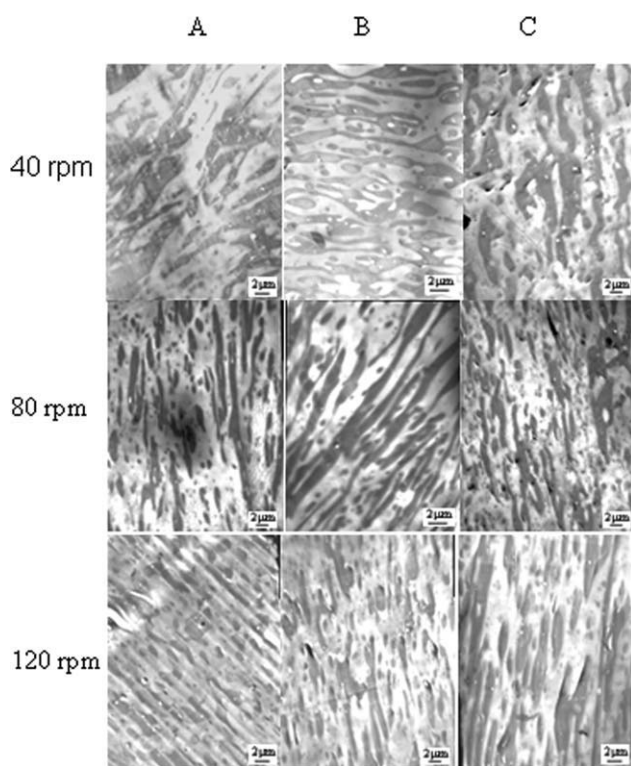
Figure 5 Morphology of 60/40 PP/PS blends during compounding in a twin-screw extruder at the rotation speeds of 40, 80, and 120 rpm, respectively.

observe a coarseness of the droplets at position C (1.2 μm). When the rotation speed is increased to 80 rpm, the droplet size increases from 0.7 μm (position A) to 0.8 (position B) and 1.0 μm (position C) along the extruder axis. At 120 rpm, the increase in the droplet size is more obvious: it increases from 0.8 μm to 1.0 and 1.5 μm.

Figure 6 presents TEM micrographs describing the morphological evolution in 90/10 PP/PS blends. At a rotation speed of 40 rpm, a coarse morphology with large PS droplets (1.0 μm) can be observed at position A. There are better dispersed PS droplets with a diameter of 0.6 μm at positions B and C. The situation is similar to that at 80 rpm. However, at 120 rpm, we can observe a morphology in which slightly elongated PS droplets are dispersed in the PP matrix, the size nearly unchanged at all positions (0.8 μm). When the rotation speed is increased to 150 rpm, the sizes of elongated and oriented PS droplets increase from 0.5 μm (position A) to 0.7 (position B) and 1.2 μm (position C). The droplet morphology can be explained on the basis of sufficient stress for disrupting the dispersed PS phase by the highly viscous PP matrix. Meanwhile, a high rotation speed leads to a high tendency to deform and coalesce, so elongated and coarse morphologies can be observed.

From Figures 5 and 6, we find that the sizes of elongated and oriented PS droplets increase at all rotation speeds for 60/40 PP/PS blends. However, for a 90/10 PP/PS blend, the size of PS droplets decreases at 40 and 80 rpm, remains constant at 120 rpm, and increases at 150 rpm along the extruder axis. As we know, at the front end of the extruder, PS melts first because of its lower flow temperature, and the mixture consists of molten PS and solid PP. However, it is very difficult for the molten PS to be dispersed by solid PP because of the much lower shear stress transfer toward it and weak dispersive forces acting on it. When solid PP begins to melt, the molten PP helps to disperse the large PS melts. Therefore, the rate of dispersion of PS depends on the rate of melting of PP. At the same time, at a very high rotation speed, the effect of the rotation speed on coalescence can be higher than that on dispersion. Thus, we think that for 90/10 PP/PS blends, the rate of dispersion of PS is higher than the rate of coalescence at 40 and 80 rpm, which is equivalent at 120 rpm and lower at 150 rpm. Otherwise, when the
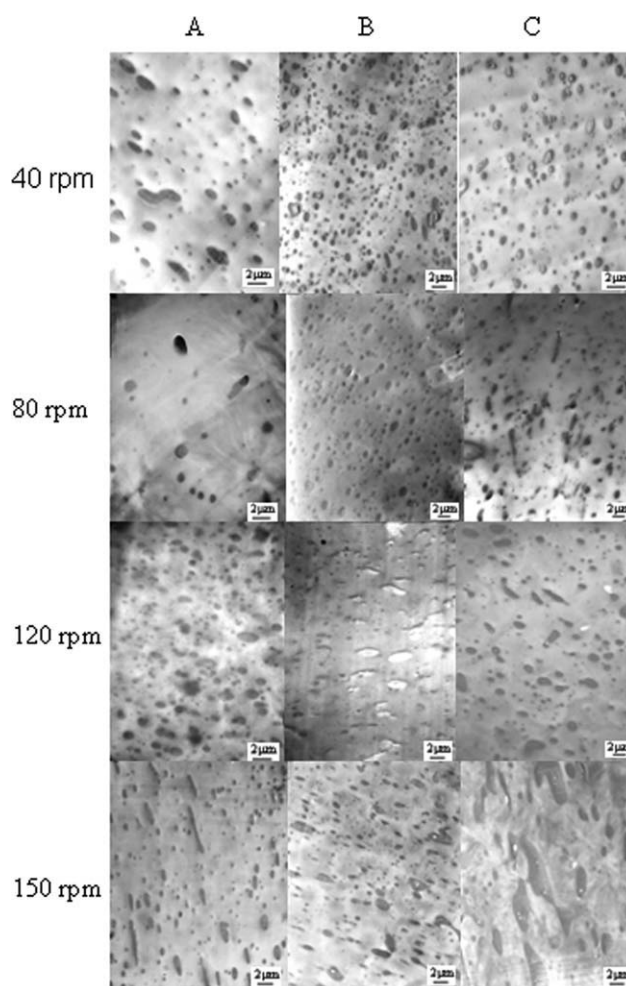

Figure 6 Morphology of 90/10 PP/PS blends during compounding in a twin-screw extruder at the rotation speeds of 40, 80, 120, and 150 rpm, respectively.
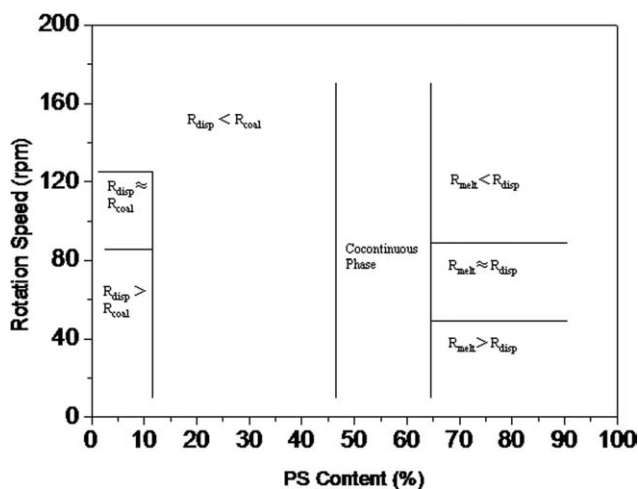
Figure 7 Schematic representation of the morphological evolution dependence of the blend compositions and rotation speeds. R_{melt}, rate of melting; R_{disp}, rate of dispersion; R_{coal}, rate of coalescence of the dispersed phase.

content of the dispersed phase is increased, there is also a higher tendency to coalesce. Thus, for 60/40 PP/PS blends, the rate of dispersion of PS is far lower than the rate of coalescence of PS particles.

According to these results, we could schematically represent the morphological evolution dependence of the blend compositions and rotation speeds as shown in Figure 7. The constituent components, rotation speeds, and blend compositions have the final influence on the morphological evolution. When PS is the major component, the rate of melting is far greater than the rate of dispersion at 40 rpm, and it is a process of size reduction for polymer melts, which is equivalent at 80 rpm. When the rotation speed is increased to 120 rpm, the rate of melting is lower than the rate of dispersion. The small droplets can coalesce with one another, so the size of the polymer melts increases. However, when PP is the major component, high rotation speeds and/or high contents of the dispersed phase lead to a high tendency to coalesce, and this might occur as a result of more chances to meet and collide for the droplets. When the blend composition is close to 1, a cocontinuous morphology is transmitted into a coarse one with an increase in the rotation speed. The viscosity ratios together with blend compositions determine the occurrence of phase inversion, as described previously.

Correlation of the morphology and mechanical properties

To investigate the correlation of the morphology and mechanical properties, a summary of the tensile strength and modulus, elongation at break, and average dispersed particle size for all the PP/PS blends is shown in Table I.

Plots of the variation of the tensile strength and tensile modulus with the weight percentage of PS are shown in Figures 8 and 9, respectively. Tensile modulus values follow a trend similar to that of the tensile strength for the blends. The value gradually decreases with the incorporation of PS, and the minimum value is reached when the PS content is 40 wt %. The reduction in the tensile strength and modulus is associated with the poor dispersion of the PS phase. It is easy to understand: the higher the content of the dispersed phase is, the more rapidly the coarsening process takes place. Thus, beyond a PS content of 60%, there is an increase in the tensile strength, and this is more obvious for the tensile modulus. This is due to the reinforcement of the PP phase by the addition of the

TABLE I
Mechanical Properties and Average Particle Sizes of the PP/PS Blends

| Blend composition	Rotation speed (rpm)	Tensile strength (MPa)	Tensile modulus (MPa)	Elongation at break (%)	Average size (μm)		
					A	B	C
PP (neat)		44.9 ± 2.9	785 ± 76	1083 ± 101	—	—	—
90/10 PP/PS	40	26.6 ± 0.5	669 ± 73	444 ± 33	1.0	0.6	0.6
90/10 PP/PS	80	28.3 ± 0.5	797 ± 81	573 ± 62	0.9	0.6	0.6
90/10 PP/PS	120	28.2 ± 1.0	708 ± 95	526 ± 51	0.8	0.8	0.8
90/10 PP/PS	150	28.6 ± 0.2	822 ± 94	654 ± 41	0.5	0.7	1.2
60/40 PP/PS	40	11.7 ± 0.3	412 ± 75	94.4 ± 6.2	0.6	0.6	1.0
60/40 PP/PS	80	14.7 ± 0.3	504 ± 60	286 ± 34	0.7	0.8	1.0
60/40 PP/PS	120	14.1 ± 0.4	517 ± 57	128 ± 25	0.8	1.0	1.5
40/60 PP/PS	40	14.2 ± 0.3	765 ± 40	2.2 ± 0.1	—	—	—
40/60 PP/PS	80	16.5 ± 3.0	725 ± 71	4.3 ± 0.3	—	0.8	0.7
40/60 PP/PS	120	16.2 ± 0.1	729 ± 96	6.7 ± 0.4	0.8	1.2	2.0
20/80 PP/PS	40	23.5 ± 0.9	1108 ± 97	5.6 ± 1.1	1.0	0.8	0.5
20/80 PP/PS	80	21.7 ± 1.3	1033 ± 96	3.6 ± 0.1	0.7	0.7	0.7
20/80 PP/PS	120	23.2 ± 1.0	1060 ± 99	3.3 ± 0.2	0.5	0.9	1.0
PS (neat)		29.0 ± 1.6	1221 ± 23	3.0 ± 0.1	—	—	—
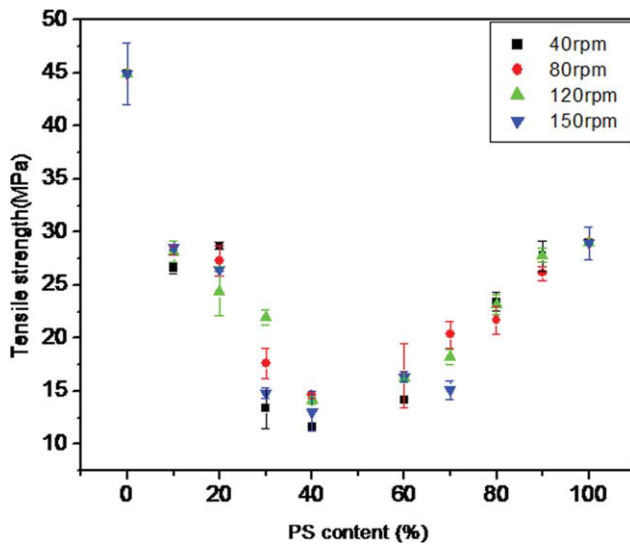
Figure 8 Variation of the tensile strength with the weight percentage of PS. [Color figure can be viewed in the online issue, which is available at wileyonlinelibrary.com.]

PS phase because PS exhibits higher tensile modulus than PP. The modulus is a measure of the strength of the material at low strains. Therefore, it can be inferred that PS-rich blends exhibit high mechanical strength. The more negative deviation can be observed in the blends with higher contents of the dispersed phase in both figures because the lower interfacial adhesion between PS and PP phases causes poorer stress transfer between the matrix and the dispersed phase. Meanwhile, the rotation speed also has an effect on the tensile strength and modulus. When PP is the major component, the values increase with an increase in the rotation speed. However, a further increase in the rotation speed may
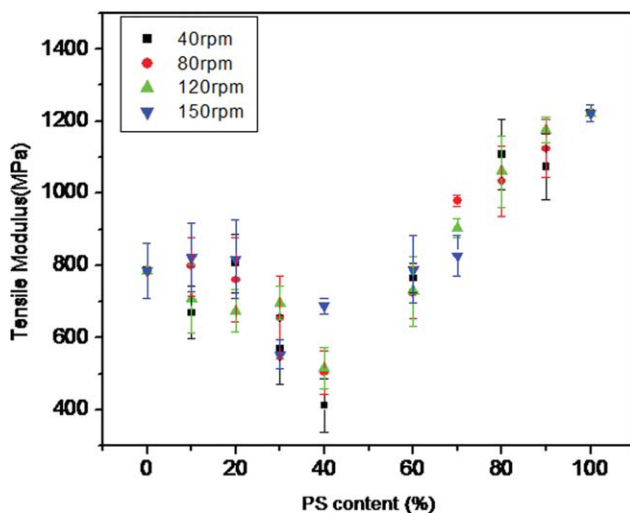
Figure 9 Variation of the tensile modulus with the weight percentage of PS. [Color figure can be viewed in the online issue, which is available at wileyonlinelibrary.com.]
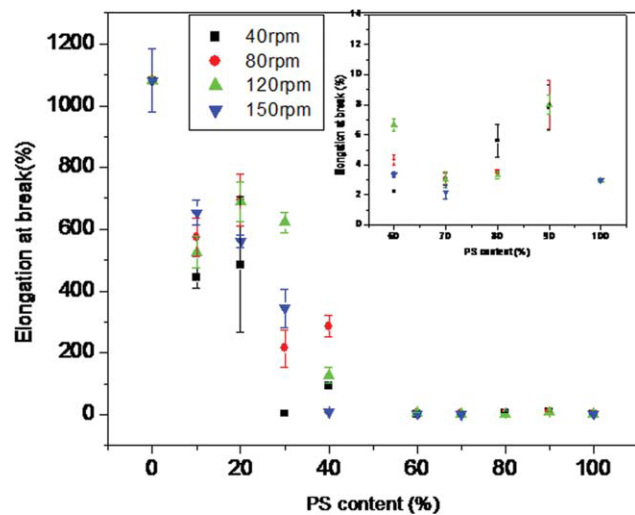

Figure 10 Variation of the elongation at break with the weight percentage of PS. [Color figure can be viewed in the online issue, which is available at wileyonlinelibrary.com.]

lead to a lower value because of the coarseness of the droplets. However, when PS is the major component, there is only a slight change due to the relatively small variation of the size and orientation of the dispersed phase.

Figure 10 shows the variation of the elongation at break as a function of the blend ratio. The elongation at break gradually decreases with PS incorporation. Beyond a PS content of 60%, the value increases slightly but remains at a low level. This is due to the better dispersion with the lower content of the dispersed phase and the continuous nature of the brittle PS phase, which is consistent with the TEM micrographs shown previously. At the same time, the rotation speed also has an effect on the elongation at break. When PP is the major component, we can observe that an elongated and oriented morphology associated with a high rotation speed favors higher elongation at break. However, a further increase in the rotation speed leads to a lower value due to the coalescence of the droplets. When PS is the major component, the elongation at break decreases slightly with an increase in the rotation speed because the increase in the size of the dispersed phase results in a smaller interfacial area, which is unfavorable for stress transfer between the matrix and the dispersed phase.

CONCLUSIONS

We have discussed the influence of the blend composition and rotation speed on the morphological evolution of PP/PS blends and proposed a possible mechanism. When PS is the major component, the rate of melting and the rate of dispersion play final roles in the morphological development of polymer melts. As soon as the rate of melting is far higher

than the rate of dispersion at a low rotation speed, it is a process of size reduction for polymer melts. However, when the rate of melting is lower than the rate of dispersion at a high rotation speed, it is a process of size enhancement. When the PP/PS blend composition is close to 1, a cocontinuous morphology is transmitted into an elongated and oriented one and then a coarse one with an increase in the rotation speed. The viscosity ratio and blend composition together determine the occurrence of phase inversion. When PP is the major component, the rate of dispersion and the rate of coalescence play key roles in morphological development. High rotation speeds and/or high contents of the dispersed phase lead to a high tendency to coalesce. There is a close correlation between the morphology and mechanical properties. The size and orientation of the dispersed phase have very important effects on the tensile strength and modulus and the elongation at break.

References

1. Utracki, L. A. Polymer Alloys and Blends—Thermodynamics and Rheology; Hanser: Munich, 1989.
2. Fortelnú, I.; Zivnú, A. Polymer 1995, 36, 4113.
3. Oshinski, A. J.; Keskkula, H.; Paul, D. R. Polymer 1996, 37, 4891.
4. Sau, M.; Jana, S. C. Polym Eng Sci 2004, 44, 407.
5. Han, C. D.; Sun, J.; Chuang, K. H.; Lee, J. K. Polym Eng Sci 1998, 38, 1154.
6. Sundararaj, U.; Macosko, C. W.; Shih, C. K. Polym Eng Sci 1996, 36, 1769.
7. Carneiro, O. S.; Covas, J. A.; Ferreira, J. A.; Cerqueira, M. F. Polym Test 2004, 23, 925.
8. He, J.; Bu, W.; Zeng, J. Polymer 1997, 38, 6347.
9. Filipe, S.; Cidade, M. T.; Wilhelm, M.; Maia, J. M. Polymer 2004, 45, 2367.
10. Machado, A. V.; van Duin, M. Polymer 2005, 46, 6575.
11. Favis, B. D. J Appl Polym Sci 1990, 39, 285.
12. Nishio, T.; Suzuki, Y.; Kojima, K.; Kakugo, M. J Polym Eng 1991, 10, 23.
13. Potente, H.; Krawinkel, S.; Bastian, M. S. S.; Potschke, P. J Appl Polym Sci 2001, 82, 1986.
14. Nair, S. V.; Oommen, Z.; Thomas, S. J Appl Polym Sci 2002, 86, 3537.
15. Sundararaj, U.; Macosko, C. W. Macromolecules 1995, 28, 2647.
16. Joseph, S.; Thomas, S. Eur Polym J 2003, 39, 115.
17. Sundararaj, U.; Macosko, C. W.; Rolando, R. J.; Chan, H. T. Polym Eng Sci 1992, 32, 1814.
18. Scott, C. E.; Macosko, C. W. Polymer 1995, 36, 461.
19. Plochocki, A. P.; Dagli, S. S.; Andrews, R. D. Polym Eng Sci 1990, 30, 741.
20. Tyagi, S.; Ghosh, A. K. Polym Eng Sci 2002, 42, 1309.
21. Lee, J. K.; Han, C. D. Polymer 1999, 40, 6277.
22. Lee, J. K.; Han, C. D. Polymer 2000, 41, 1799.
23. Li, H.; Hu, G. H. J Polym Sci Part B: Polym Phys 2001, 39, 601.